Published 03/28/2017

doi:10.4271/2017-01-0586
saecomveh.saejournals.org

An Application of a Model-Prediction-Based Reference Modification Algorithm to Engine Air Path Control

Hayato Shirai, Hayato Nakada, Akio Matsunaga, and Hiroyuki Tominaga
Toyota Motor Corporation

ABSTRACT

In real-world automotive control, there are many constraints to be considered. In order to explicitly treat the constraints, we introduce a model-prediction-based algorithm called a reference governor (RG). The RG generates modified references so that predicted future variables in a closed-loop system satisfy their constraints. One merit of introducing the RG is that effort required in control development and calibration would be reduced. In the preceding research work by Nakada *et al.,* only a single reference case was considered. However, it is difficult to extend the previous work to more complicated systems with multiple references such as the air path control of a diesel engine due to interference between the boosting and exhaust gas recirculation (EGR) systems. Moreover, in the air path control, multiple constraints need to be considered to ensure hardware limits. Hence, it is quite beneficial to cultivate RG methodologies to deal with multiple references and constraints. In this paper, we develop the RG algorithm based on gradient descent method to allow for multiple references and constraints. We demonstrate the effectiveness of the presented RG algorithm in a transient driving cycle experiment using a real engine, in which constraints are enforced on maximal boost pressure, turbine speed, compressor surge and maximal and minimal EGR rates. The experiment implies that we have expanded the applicability of an RG to system with multiple references compared to the previous work for only a single reference.

CITATION: Shirai, H., Nakada, H., Matsunaga, A., and Tominaga, H., "An Application of a Model-Prediction-Based Reference Modification Algorithm to Engine Air Path Control," *SAE Int. J. Commer. Veh.* 10(1):2017, doi:10.4271/2017-01-0586.

INTRODUCTION

Environmental concerns such as global warming and air pollution, as well as the limitation of energy resources, have been prompting calls for cleaner emissions and greater fuel efficiency in automobiles. At the same time, even as automobile engine systems continue to increase in complexity, they are expected to maximize the potential output, fuel efficiency, and emissions performance. Achieving such maximization increases the necessity for precise control near several constraints on the engine. For example, the engine air path system considered in this paper involves hardware-based constraints on the admissible upper limit of state variables such as boost pressure (intake manifold pressure) or turbine speed, as well as limits on the actuators. In the actual development of control systems, satisfying such constraints involves repeated testing to determine constants and maps in the control algorithms. As engine hardware becomes more complex, the number of constraints that must be taken into account is likely to rise. The increase in the complexity of control algorithms is expected to increase the time required to develop control algorithms and determine the constants and the maps. In this context, control technologies aimed at enforcing constraints are attracting attention.

Control technologies that can take state variable and control input constraints into account include anti-windup control (AWC) [2] and reference governors (RG) [3]. The AWC control method takes account of saturation constraints for control input and suppresses excessive windup from integral compensation in a PID control, but it cannot directly deal with constraints in state variables. In contrast, RG-based methods generate modified references so that predicted future variables in a closed-loop system satisfy their constraints as shown in Figure 1. In the RG, an objective function considering predicted constraint satisfaction (the constraint penalty) is minimized, resulting in the optimal modified reference. Introducing the RG provides the following three benefits.

1. The ability to operate near the constraints is expected to improve control performance.
2. An existing feedback controller can be combined with the RG.
3. It is expected that constraint enforcement and calibration effort to determine constants and maps can be reduced.

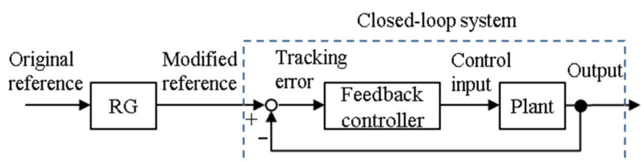

Figure 1. Control system with a reference governor (RG)

Among preceding research works related to RG, there were several application studies reported such as the application to a helicopter [3], a high pressure steam condenser [4] and a turbocharged automotive engine [5]. In the past, the authors of [6,7] have proposed RG algorithms for a single-variable reference and applied to diesel engine control systems, in particular, catalyst temperature control [6] and boost pressure control [7]. Applying the RGs to more complex systems that include multiple control inputs and outputs as in air path systems will require expanding them to cover multiple references. This will undoubtedly make RG algorithms even more complex. In such a case, the computational burden has to be kept under a level of current engine electronic control units (ECUs). This paper therefore proposes an online RG algorithm executable on the ECU to simultaneously modify multiple references. By applying the algorithm to the control of boost pressure and exhaust gas recirculation (EGR) in a diesel engine air path system, we validate the effectiveness of the present method.

SYSTEM CONFIGURATION

Figure 2 illustrates the structure of a diesel engine air path system. A variable geometry turbocharger (VGT) is used to achieve the boost pressure required for both particulate matter reduction and engine power generation. At the same time, an EGR valve and a throttle are used to recirculate some of the exhaust emissions to the intake and reduce nitrogen oxides (NO*x*) emissions. The air path can be described as an interactive system, since exhaust energy is transmitted through the turbine shaft and the exhaust gas goes through the EGR path to the intake path. We define the EGR rate in the intake manifold as the ratio of the exhaust gas flow rate passing through the EGR valve to the mixed gas flow rate into the cylinder. The two variables, boost pressure and the EGR rate, have to be controlled simultaneously due to their interference.

The constraints in the plant are presented below. First, boost pressure is subject to an upper limit constraint due to the allowable maximum cylinder pressure during turbocharging. The EGR rate is constrained at upper and lower limits, since the upper one is for stable combustion, and the lower for a NO*x* reduction requirement. There are also a number of other constraints in reality (see Table 1).

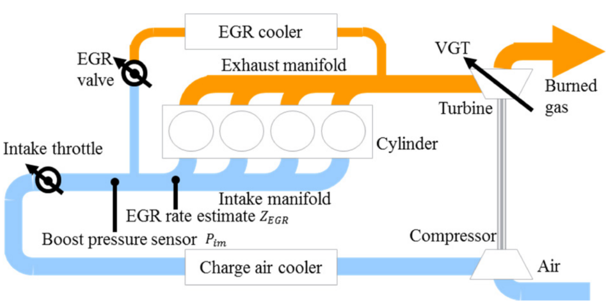

Figure 2. Air path system of a diesel engine

STRUCTURE OF REFERENCE GOVERNOR

The entire structure of the RG algorithm is shown in Figure 3. By repeating the iteration loop consisting of elements 1 to 3 in the figure, we can calculate the modified references in real time. An overview of the elements 1 to 3 is as follows

1. Model-based future prediction: A model of the closed-loop system surrounded by the dashed rectangle in Figure 1 is used to predict the future behavior of state variables over a prescribed prediction horizon.
2. Calculation of an objective function: The predicted state variables over the prediction horizon are used to calculate an objective function that takes the constraint penalty into account.
3. Search for modified references: An iterative search for modified references is carried out to minimize the objective function. Since this paper considers a tracking control for the two references, namely, boost pressure and the EGR rate, an optimization algorithm on a planar space is required.

The next section provides details on these three elements in the RG algorithm.

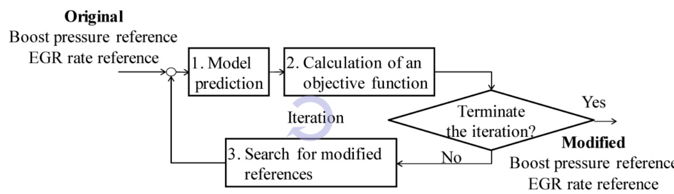

Figure 3. Structure of the RG algorithm

PLANT MODELING

In this section, we consider modeling the diesel engine air path system. Table 1 lists the main constraints on the plant. The characteristics of constraints are categorized according to the following characteristics.

1. Whether a constraint is on a single variable ((i) to (iii)), or is affected by multiple variables (iv).
2. Whether a constraint is a time-driven event ((i) and (ii)) or a crank angle-driven event dependent upon the engine speed (iii).
3. Among time-driven events, whether it (i) involves a fast phenomenon (time constant of 1 second or less) through the direct effect of gas flow, or (ii) involves a slower phenomenon (time constant of more than 1 second) due to the effect of a change in energy or a transfer of heat.

Table 1. Constraints in the air path system

Category	Single variable			(iv)Multiple variables
	Time-driven event		(iii)Crank angle-driven event	
	(i)Fast response	(ii)Slow response		
Constraint	・EGR rate ・Boost pressure ・Exhaust pressure ・Turbine speed	・Compressor outlet temperature ・Exhaust gas temperature	・Missfire ・Cylinder pressure	・Compressor surge

The above points are used to divide the constraints into the four categories as shown in Table 1. It is important to develop an RG algorithm that covers all of those categories (i) to (iv). In this paper, we select the boost pressure P_{im} , the EGR rate Z_{EGR}, the exhaust pressure (the pressure inside the exhaust manifold) P_{exh} and the turbine speed N_T constraints from category (i). In addition, the compressor surge constraint is considered category (iv). Categories

(ii) and (iii) are single-variable constraints and omitted here for the sake of simplicity, because they can be extended in the same manner as the category (i). Unlike the categories (i) to (iii), the surge constraint in the category (iv), is affected by multiple variables. To handle this, we need to deal with a constraint on multi-dimensional space in the RG algorithm as described below.

Figure 4 outlines the surge constraint. The surge limit line l is defined on a planar space of G_a and P_r, where G_a is the air flow rate, $P_r = P_3/P_a$ is a pressure ratio, P_3 is the compressor outlet pressure and P_a is the ambient pressure. The surge occurs in the operating region on the upper-left of l. It depends on both G_a and P_r, so these two variables should be considered simultaneously. For the sake of simplicity, this paper assumes the ambient pressure P_a is constant, and models the compressor outlet pressure P_3 rather than P_r.

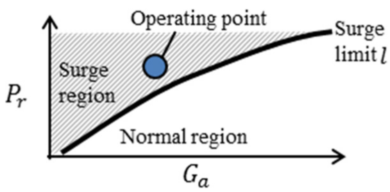

Figure 4. Schematic diagram of compressor surge

We introduce a discrete time plant model described by

$$x(k+1) = Ax(k) + Bu(k) + Ed(k), \tag{1}$$

where $x = [P_{im}\ Z_{EGR}\ P_{exh}\ N_T\ G_a P_3]^T \in \mathrm{R}^6$ is the state vector, $u = [u_{vgt}\ u_{egr}\ u_{thr}]^T \in \mathrm{R}^3$ is the input vector whose elements are, in order, the VGT, the EGR valve and the throttle positions. $d = u_{fuel} \in \mathrm{R}$ is the fueling command. k represents discrete time. $A \in \mathrm{R}^{6\times6}$, $B \in \mathrm{R}^{6\times3}$ and $E \in \mathrm{R}^{6\times1}$ are coefficient matrices. Note that although Equation (1) is written as a linear dynamical model, the characteristics of actual engines vary according the operating region. Therefore, the matrices A, B and E are described as functions of engine speed N_e and the fueling u_{fuel}. In the RG, Equation (1) is used as the future prediction model. Since the future values of N_e and u_{fuel} are unknown over the prediction horizon, they are assumed to be constant over it.

In this paper, we utilize a PI controller as the feedback controller in Figure 1. By applying the PI controller to the plant model, we obtain the closed-loop system. In the RG design described in the following section, a model of the closed-loop system is used to predict the future behavior of state variables over a prescribed prediction horizon.

REFERENCE GOVERNOR DESIGN

This section introduces an objective function involving a constraint penalty over the prediction horizon, and designs an RG algorithm to minimize the function. In particular, the surge constraint, which depends on two states, is taken into account by expanding the one-dimensional penalty as in [6, 7] to a multi-dimensional one (two-dimensional in this case).

Constraint Penalty on Multi-Dimensional Space

Constraint penalties on a prediction horizon are examined below. As shown in Figure 5, the constraint penalty in [7] is given as the area of a single predicted trajectory over its constraint. Now, we extend the constraint penalty to a two-dimensional one to deal with the surge constraint, which depends on two states.

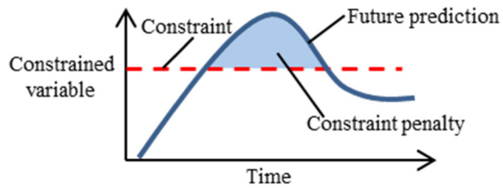

Figure 5. Constraint penalty for a single variable

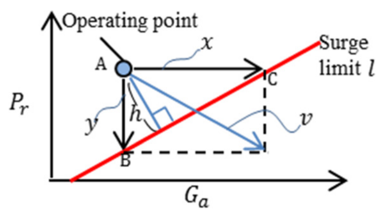

Figure 6. Definition of constraint penalty in 2-dimensional plane

Figure 6 is a conceptual diagram of the two-dimensional constraint penalty. Here, $x \in \mathrm{R}^2$ is a vector from a prescribed operating condition A to the intersection C projected along the axis of air flow rate G_a. Similarly, $y \in \mathrm{R}^2$ is a vector from A to B along the axis of pressure ratio P_r. The surge limit line l in the graph is approximated as a straight line near the operating condition A. Then, the distance h between the operating condition A and the surge limit line l is a possible candidate for the constraint penalty. Considering the area of triangle ABC yields $h = \|x\|\|y\|/\sqrt{\|x\|^2 + \|y\|^2}$. In the denominator on the right-hand side, x and y vary in time, which could cause a division by zero in online calculation. As an alternative, the norm of the vector $v = x + y$, namely $\|v\| = \sqrt{\|x\|^2 + \|y\|^2}$, is therefore considered. Although $\|v\|$ could have a value larger than the distance h, it is expected that by minimizing the alternative $\|v\|$ the distance h can be minimized as well without causing a division by zero. In this paper, $\|v\|$ is regarded as the constraint penalty for the surge constraint.

Note that the constraint penalty calculation above gives a low computation burden, since a straight line approximation is introduced near the operating condition of the surge limit line. Of course, a complex calculation such as evaluating the area between a more complicated surge curve and a predicted trajectory could be a possible choice, when constraints with more complex shapes are handled or more rigorous constraint penalties are evaluated. However, such cases may lead to a significantly increased computation burden. Hence, it is necessary in reality to determine a method of calculating constraint penalties by considering the trade-offs between the allowable computation burden on ECUs and the evaluation accuracy for constraint penalties.

Objective Function

The modified reference w that minimizes the constraint penalty is calculated based on the objective function $J(w)$ described by

$$J(w) = \|r - w\|^2 + \sum_{l=1}^{5} \psi_l J_l^2, \tag{2}$$

where

$$J_1 = \sum_{k=1}^{N_h} \max\{P_{im}(k) - \bar{P}_{im}, 0\},$$

$$J_2 = \sum_{k=1}^{N_h} \max\{P_{exh}(k) - \bar{P}_{exh}, 0\},$$

$$J_3 = \sum_{k=1}^{N_h} \max\{N_T(k) - \bar{N}_T, 0\},$$

$$J_4 = \sum_{k=1}^{N_h} \max\left\{\|Z_{EGR}(k) - Z_{EGRref}\| - \frac{\bar{Z}_{EGR}}{2}, 0\right\},$$

$$J_5 = \sum_{k=1}^{N_h} \sqrt{\left[\max\left\{\frac{\underline{G_a} - G_a(k)}{\underline{G_a}}, 0\right\}\right]^2 + \left[\max\left\{\frac{P_r(k) - \bar{P}_r}{\bar{P}_r}, 0\right\}\right]^2}.$$

Here, the first term of $J(w)$ implies the minimization of the distance between the original reference r and a modified reference w. The second term represents minimizing constraint penalties. Here, J_1, J_2, J_3 are the constraint penalties for the boost pressure P_{im}, the exhaust pressure P_{exh}, and the turbine speed N_T, respectively. J_4 represents the constraint penalty for the upper and lower limit constraints on the EGR rate. It is intended to keep the EGR rate response within a banded area of width $\bar{Z}_{EGR}$ around the EGR rate reference Z_{EGRref}. In addition, J_5 represents the penalty for the surge constraint. Note that the two-dimensional constraint penalty as described in the previous subsection is applied. $\psi_l (l = 1,\ldots,5)$ are scalar weighting coefficients, $N_h \in \mathrm{N}$ is the prediction horizon. $\bar{P}_{im}$, $\bar{P}_{exh}$, $\bar{N}_T$ and $\bar{P}_r$ are prescribed upper limits on P_{im}, P_{exh}, N_T, and P_r, respectively. $\underline{G_a}$ stands for a given lower limit on G_a. Here, $\bar{P}_r$ and $\underline{G_a}$ are functions of P_r and G_a, therefore varied over the prediction horizon.

In this paper, we use the objective function $J(w)$ based on the idea of soft constraint. Hence, there is a possibility that a constraint is not met. If we introduce a marginal constraint compared to the original one, then the original constraint can be enforced. This should be checked by simulations and tests in reality.

Optimization Algorithm

An online reference modification algorithm is developed based on the gradient descent method [9] that is a typical multi-dimensional optimization method. The gradient descent method yields the following update law to obtain the optimum iteratively.

$$w^{(m+1)} = w^{(m)} - \alpha \nabla J\left(w^{(m)}\right), \quad m = 0, 1, \ldots, M-1, \tag{3}$$

where $w^{(m)} \in \mathrm{R}^2$ is the modified reference candidate in the m-th iteration $\alpha \in \mathrm{R}$ is a coefficient, and $\nabla J(w^{(m)}) \in \mathrm{R}^2$ represents the gradient with respect to $w^{(m)}$. Performing the iterative computation in Equation (3) makes it possible to simultaneously modify multiple references in real time. Figure 7 shows a calculation process. Each step of the calculation is outlined below.

Step 1: The initial modified reference candidate is set to $w^{(0)} := r$. The objective function $J(w)$ is then used to calculate the gradient $\nabla J(w^{(0)})$ (as in the Appendix A).

Step 2: Based on Equation (3), we search for a local minimum $W^{(1)}$ in the direction $-\nabla J(w^{(0)})$. The search is conducted based on the bisection search method [6].

Step 3: Similarly, the gradient $\nabla J(w^{(1)})$ is computed for the modified reference candidate $W^{(1)}$.

The locally optimal modified reference $W^{(M)}$ is obtained by repeating Steps 2 and 3 in M times. The entire RG algorithm [10] is shown in Appendix B.

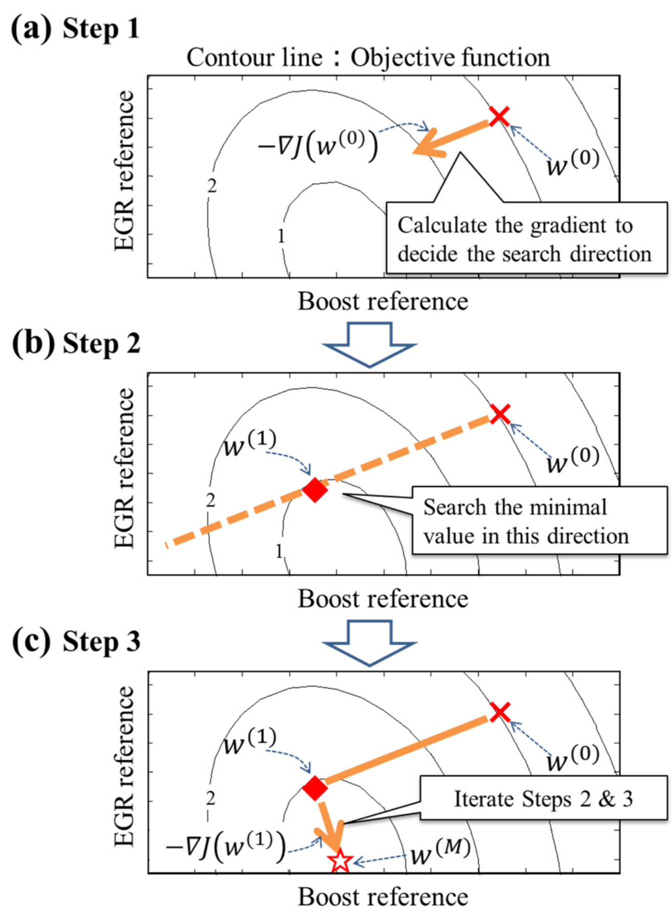

Figure 7. Gradient descent algorithm

EXPERIMENT RESULT

This section shows experimental results of applying the RG algorithm to a 4-cylinder 3.0 [L] diesel engine. The experiments were conducted on a transient test cell to simulate vehicle running. The RG algorithm was implemented as C program generated by Matlab/ Simulink and embedded on the ECU.

System Identification

System identification was performed to determine coefficient matrices *A B* and *E* in Equation (1). Figure 8 shows the time sequences of input signals, which are generated as the pseudo random binary sequence (PRBS) typically used in system identification [8]. Based on the least squares method [8] the coefficient matrices were identified. Figure 9 shows the result. Regarding the operating condition, the engine speed was fixed at 2,000 [rpm], and the fueling was set to vary randomly centering on 25 [mm^3/stroke]. The figure also shows the R-squared (R^2) figures to see the goodness-of-fit. The values of R^2 were over 70 [%]. Similar identification experiments were conducted under different operating conditions, and prediction models were built in a similar manner to cover the entire operating region.

As a note, the linear model form Equation (1) was used in this paper. However, a nonlinear model could be adopted if a more accurate prediction would be required. In such a case, the computation burden required for the RG algorithm could be increased. Hence, it is necessary to determine the model structure by considering the tradeoffs between model accuracy and the computation burden on ECU.

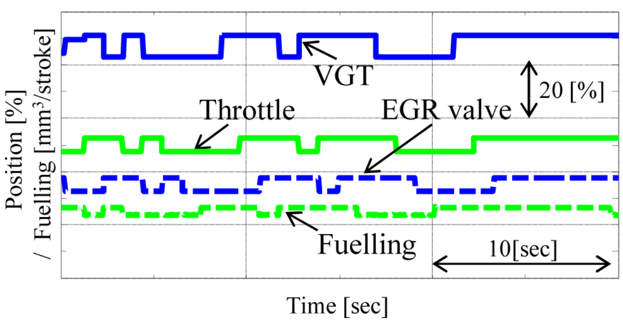

Figure 8. Input data for system identification

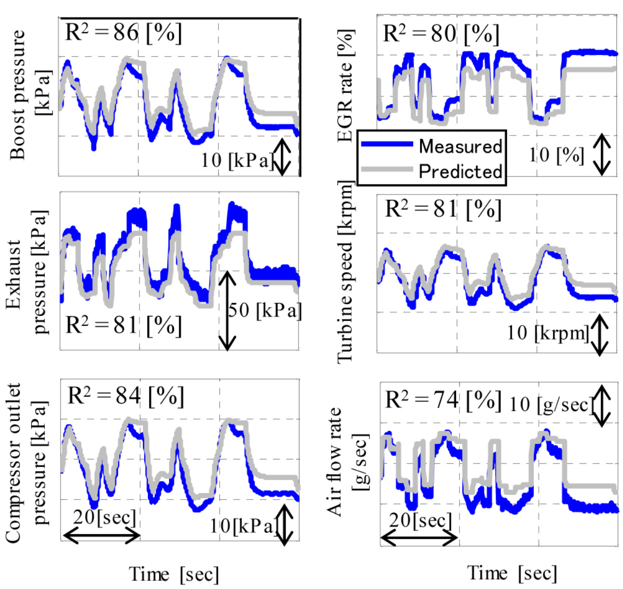

Figure 9. Model validation results

Simulation Result

Figure 10 shows a simulation result to verify the behavior of the control system with the RG. Note that hypothetical constraint values were set differently from those of production control in this simulation to validate the effectiveness of the RG algorithm proposed. The engine speed was fixed at 2,000 [rpm] and the fueling command was fixed at 25 [mm^3/stroke]. The boost pressure and the EGR rate references were changed in steps. Without the RG, the area A in the figure shows a violation with the boost pressure constraint, while with the RG, the boost pressure reference is modified downward and moves to satisfy the constraint. Similarly, the area B in the figure, the lower limit constraint of the EGR rate is satisfied with the RG rather than without it. In this way, the simulation result confirms the effectiveness of the proposed RG algorithm.

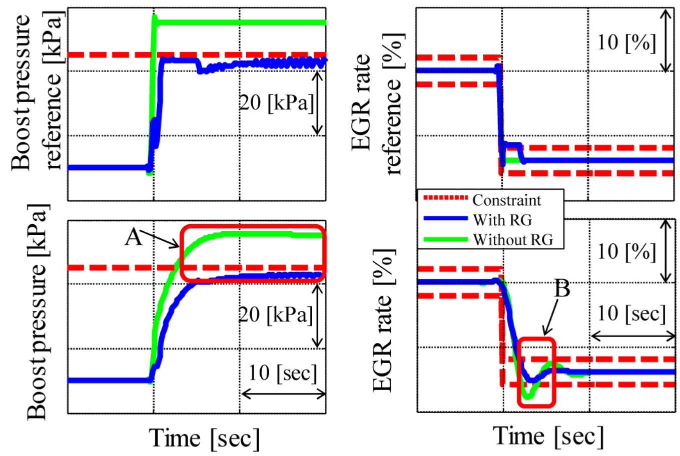

Figure 10. Comparison of simulation results with/without RG

Result of Actual Engine Experiment

An experiment based on the Worldwide harmonized Light duty Test Cycle (WLTC) was conducted on a transient test cell. Note that hypothetical constraint values were set differently from those of production control in this experiment to validate the effectiveness of the RG algorithm proposed. Figure 11 shows the result. The area A in the figure shows that with the RG, both the boost pressure and the EGR rate references are modified downward and the boost pressure constraint is satisfied better than the case without RG. Similarly, in the area B, results relative to the upper limit constraint of the EGR rate are better with the RG than the case without it. Next, Figure 12 shows the results for the surge constraint. Without the RG, the surge limit line represented by the dashed line reaches the upper left side of the surge region, while with the RG, the constraint penalty is reduced. Figure 13 presents a comparison of the constraint penalties. Here, the constraint penalties without the RG are normalized at 100 [%]. While the EGR rate constraint shows a room for improvement, all constraints are better satisfied. In addition, the computation time in this experiment was approximately 30 [msec].

The above indicates that the RG algorithm for multiple references is also valid for transient operations with actual engines.

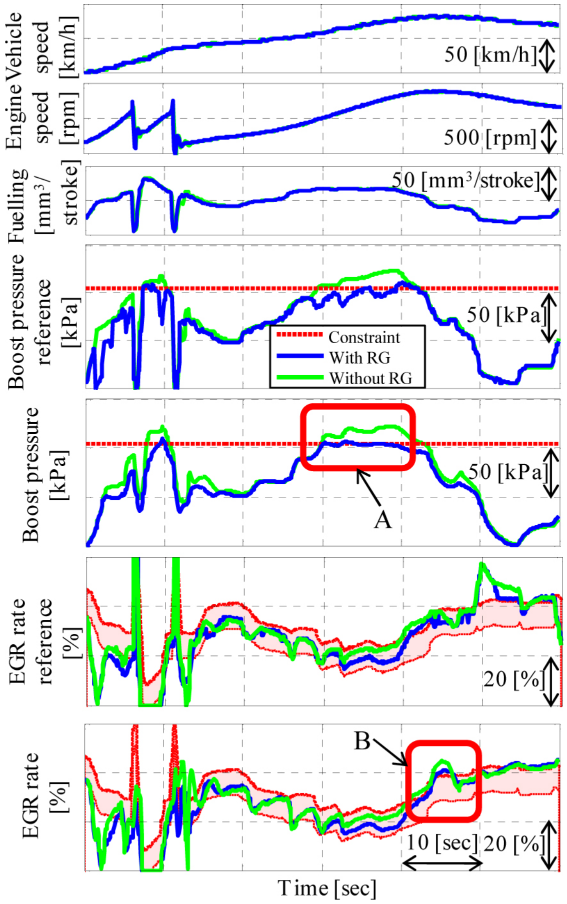

Figure 11. Comparison of transient experiment results

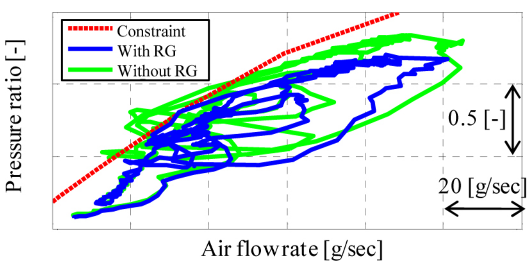

Figure 12. Comparison of results for surge constraint

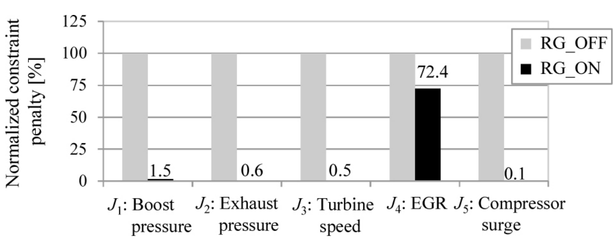

Figure 13. Comparison of constraint penalties

Tracking Performance Improvement with RG

It can be expected that introducing the RG to a conventional control would give an improvement of tracking performance both in the boost pressure and the EGR rate. The RG was therefore applied after modifying feedback gains in the conventional control system to get a quick response. Note that the conventional control was calibrated manually to enforce the constraints. Figure 14 shows a comparison of resulting boost pressure responses. The operating condition was set to the engine speed of 1,500 [rpm] and a stepped change of the fueling from 55 to 85 [mm³/stroke]. The left-hand plot in Figure 14 shows the boost pressure reference and modified reference, while the right-hand plot represents their respective actual boost pressure. The area A in the figure shows that the RG improves the rise time compared to the conventional control by 0.7 [sec]. In addition, comparing the integral value of the reference tracking error shows an improvement of approximately 7[%] for the RG over the conventional control.

Similarly, Figure 15 compares results from the EGR control. The operating conditions were set to the engine speed of 2,000 [rpm] and a stepped fueling change from 55 to 25 [mm³/stroke]. The area B in the right-hand plot shows an improvement of approximately 14 [%] in the EGR rate overshoot for the system with the RG compared to the conventional control. Moreover, comparing the integral value of the reference tracking error shows an improvement of approximately 8 [%] for the RG over the conventional control.

The above experimental results indicate that the RG algorithm is potentially effective to improve tracking performance with a quick transient response.

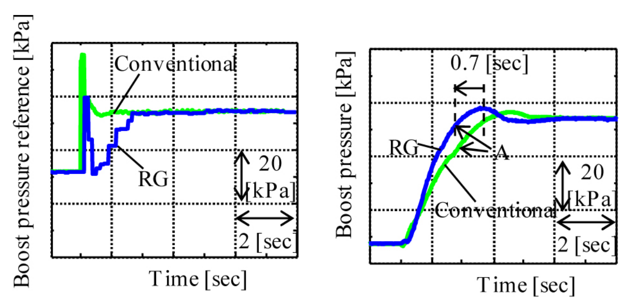

Figure 14. Comparison of boost pressure responses

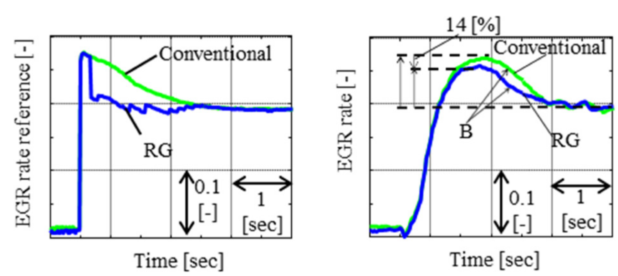

Figure 15. Comparison of EGR rate responses

CONCLUSION

This paper has been devoted to the application of RGs to engine air path systems. An algorithm to calculate modified references based on the gradient descent method has been proposed to modify multiple references, namely, both boost pressure and the EGR rate references. Experiments using a real engine have showed the effectiveness of the present method, particularly with regard to better satisfying constraints and improving tracking performance.

In terms of control engineering, the present research is significant from the following perspectives:

1. The paper has expanded the applicability of RG methods to a single reference from past research [6, 7] to simultaneously account for multiple references.
2. A method to deal with constraints depending on multiple state variables has been proposed and validated in the surge constraint case. This enables to similarly expand the method to high-dimensional complicated constraints.

Consequently, this research has established a more versatile constraint enforcement control technology and expanded the range of plants to which RG algorithms can be applied.

Moreover, the proposed RG algorithm can conceivably be expanded to a higher accuracy algorithm by, for example, using nonlinear prediction models or constraints. In such a case, computational burden could increase. The model precision, evaluation of constraint penalties and iteration numbers in the RG algorithm could be compromised in reality. Therefore, the check of computational feasibility and the resulting control performance are always required.

One potential further research topic is to consider how to satisfy multiple constraints when more constraints are considered. In addition, although this paper has focused especially on the boost pressure and the EGR rate, their effects on engine performance aspects such as power generation or exhaust performance must still be clarified.

REFERENCES

1. Niimi, K., “New Development of Industrial Applications of Model Predictive Control,” Journal of The Society of Instrument and Control Engineers, 43(9):647–653,2004.
2. Wada, N. and Saeki, M., “Anti-windup Control of Systems with Input Saturation,” Systems, control and information 46(2):84–90, 2002.
3. Kogiso, K., Minemura, H. and Hirata, K., “Verification of Reference Governor Control Approaches to Experimental Systems with Control Constraints,” Transactions of the Japan Society of Mechanical Engineers Series C 69(681): 1238–1246, 2003.
4. Hatanaka, T., Ase, H., Takaba, K. and Katayama, T., “Control of High-pressure Steam Condenser via Reference Governor,” Transactions of the Institute of Systems, Control and Information Engineers 29(7):275–282, 2007.
5. Kolmanovsky, I., Garone, E. and Cariano, S.D., “Reference and Command Governors: A Tutorial on Their Theory and Automotive Applications,” Proceedings of the 2014 American control Conference, 226–241, 2014.
6. Nakada, H., Milton, G., Martin, P., Iemura, A. and Ohata, A., ”Reference Management for Aftertreatment Temperature Control of Automotive Diesel Engines,” Proceedings of 2012 IFAC Workshop on Engine and Powertrain Control, Simulation and Modeling, Volume 3(1), 373–383, 2012, doi:10.3182/20121023-3-FR-4025.00003.
7. Nakada, H., Martin, P., Milton, G., Iemura, A. and Ohata, A., “An Application Study of Online Reference Governor to Boost Pressure Control for Automotive Diesel Engines,” Proceedings of 2014 American Control Conference, 3135–3140,2014, doi:10.1109/ACC.2014.6858582.
8. Ljung, L., “System identification theory for the user,” (New Jersey, Prentice-Hall, 1987), 361–373, ISBN:0-13-881640-9.
9. Fukushima, M., “Introduction to Mathematical Programming,” (Tokyo, Asakura Shoten, 1996), 96–109, ISBN:978-425480043.
10. Nakada, H., Martin, P., Wijesinghe, A., Shirai, H., Matsunaga, A., Tominaga, H., “An Application of Reference Governor to a Diesel Engine Air Path System: Implementation of a MultiVariable Reference Modification Algorithm,” presented at 8th IFAC Symposium on Advances in Automotive Control AAC 2016, Sweden, June, 20–23, 2016.

CONTACT INFORMATION

Hayato Shirai
TOYOTA MOTOR CORPORATION
Higashifuji Technical Center
1200, Mishuku, Susono, Shizuoka, 410-1193 Japan
hayato_shirai@mail.toyota.co.jp

ACKNOWLEDGMENTS

The authors would like to thank Dr. Peter Martin, Mr. Anuradha Wijesinghe, Dr. Gareth Milton, Dr. Peter Fussey, Dr. Antony John Truscott (Ricardo UK Ltd.) and Mr. Takeshi Iwanami (Ricardo Japan Ltd.) for their valuable comments on algorithm design and experiments.

DEFINITIONS/ABBREVIATIONS

RG - reference governor

EGR - exhaust gas recirculation

AWC - anti-windup control

ECU - engine control unit

VGT - variable geometry turbocharger

NO_x - nitrogen oxides

PRBS - pseudo random binary sequence

WLTC - worldwide harmonized light duty test cycle

APPENDIX

APPENDIX A: GRADIENT CALCULATION IN OPTIMIZATION ALGORITHM

Here, we show how to calculate the gradient $\nabla J(w^{(m)})$ in the gradient descent algorithm.

The modified reference candidate obtained in the -th iteration is defined as

$$w^{(m)} = \begin{bmatrix} w_P^{(m)} \\ w_E^{(m)} \end{bmatrix},$$

where $w_P^{(m)}$ and $w_E^{(m)}$ are the modified reference candidates for boost pressure and the EGR rate respectively. The four neighborhood of $W^{(m)}$ points with the distance $\Delta \epsilon$ R along each axis are defined by

$$w_u^{(m)} = \begin{bmatrix} w_P^{(m)} \\ w_E^{(m)} + \Delta \end{bmatrix}, w_d^{(m)} = \begin{bmatrix} w_P^{(m)} \\ w_E^{(m)} - \Delta \end{bmatrix}, w_r^{(m)} = \begin{bmatrix} w_P^{(m)} + \Delta \\ w_E^{(m)} \end{bmatrix}, w_l^{(m)} = \begin{bmatrix} w_P^{(m)} - \Delta \\ w_E^{(m)} \end{bmatrix}. \tag{4}$$

The gradient $\nabla J(W^{(m)})$ is approximately computed by

$$\nabla J(w^{(m)}) \approx \frac{1}{2\Delta} \begin{bmatrix} J\left(w_r^{(m)}\right) - J\left(w_l^{(m)}\right) \\ J\left(w_u^{(m)}\right) - J\left(w_d^{(m)}\right) \end{bmatrix}. \tag{5}$$

APPENDIX B: RG ALGORITHM

In this appendix, we show the RG algorithm as below.

1. $m := 0$, $w^{(m)} := r(K)$
2. While $m \leq m_{max}$
3. Compute $w_j^{(m)}$ $\forall j \in \{u,d,r,l\}$ by (4)
4. Compute $J\left(w_j^{(m)}\right)$ $\forall j$
5. Compute $\nabla J(w^{(m)})$ by (5)
6. % Search a local minimum in the direction of the gradient $\nabla J(W^{(m)})$ via a bisection search
7. $p := 0$, $\alpha_{min}^{(p)} := \alpha_{min}$, $\alpha_{max}^{(p)} := \alpha_{max}$
8. While $p \leq p_{max}$
9. $\alpha_{mid}^{(p)} := (\alpha_{min}^{(p)} + \alpha_{max}^{(p)})/2$
10. $w_q^{(p)} := w^{(m)} + \alpha_q^{(p)} \nabla J\left(w^{(m)}\right)$ $q \in \{min.mid.max\}$
11. Align$J\left(w_q^{(p)}\right)$, $q \in \{min.mid.max\}$ in the ascending order
12. Discard the largest$J\left(w_q^{(p)}\right)$ and align the remaining two in the ascending order in $\alpha_q^{(p)}$
13. $\alpha_{min}^{(p+1)}$ is set to the smaller $\alpha_q^{(p)}$
14. $\alpha_{max}^{(p+1)}$ is set to the larger $\alpha_q^{(p)}$
15. $P := P + 1$
16. end
17. $\alpha^{(m)} := \alpha^{(p_{max})}$
18. $w^{(m+1)} := w^{(m)} - \alpha^{(m)} \nabla J(w^{(m)})$, $m := m + 1$
19. end
20. $w^* := w^{(m_{max})}$.

Here, α_{min}, α_{max} ϵ R are given constants representing a search range for $\alpha^{(m)}$. $p_{max;}$ ϵ N represents a given constant implying the maximal iteration number of the bisection method. $w^* \in R^2$ is the optimal modified reference obtained from the RG algorithm.